Title: The intrinsic neonatal hippocampal network: rsfMRI findings

Abbreviated Title: The intrinsic neonatal hippocampal network

Authors:

Athena L. Howell (contribution: running registration and fMRI analyses, statistical analyses and writing the manuscript),

David E. Osher (preprocessing fMRI data and editing the manuscript),

Jin Li (preprocessing fMRI data and editing the manuscript),

and Zeynep M. Saygin (PI/advisor, guiding the research and analyses, checking results and editing the manuscript)

The Ohio State University, 43210

Please address correspondence to:

Athena L. Howell, The Ohio State University, 225 Psychology Building, 1835 Neil Avenue, Columbus, OH, 43210. E-mail: howell.551@osu.edu

# of pages: 19 (in body of manuscript)

# of Figures: 5 Figures

# of words in abstract: 201

# of words in introduction: 575

# of words in discussion: 1077

Acknowledgements; The authors declare no competing financial interests

Abstract

Many adults cannot voluntarily recall memories before the ages of 3-5, a phenomenon referred to as "infantile amnesia". The development of the hippocampal network likely plays a significant part in the emergence of the ability to form long-lasting memories. In adults, the hippocampus has specialized and privileged connections with certain cortical networks, which presumably facilitate its involvement in memory encoding, consolidation, and retrieval. Is the hippocampus already specialized in these cortical connections at birth? And are the topographical principles of connectivity (e.g. long-axis specialization) present at birth? We analyzed resting-state hippocampal connectivity in neonates scanned within one week of birth (Developmental Human Connectome Project) and compared them to adults (Human Connectome Project). We explored the connections of the whole hippocampus and its long-axis specialization to seven canonical cortical networks. We found that the neonatal hippocampal networks show clear immaturity at birth: adults showed hippocampal connectivity that was unique for each cortical network, whereas neonates showed no differentiation in hippocampal connectivity across these networks. Further, neonates lacked long-axis specialization (i.e., along anterior-posterior axis) of the hippocampus in its differential connectivity patterns to the cortical networks. This immaturity in connectivity may contribute to immaturity in memory formation in the first years of life.

50 “New and Noteworthy”:

51 While animal data, and anatomical and behavioral human data from young children
52 suggest that the hippocampus is immature at birth, to date, there are no direct assessments of
53 human hippocampal functional connectivity (FC) very early in life. Our study explores the FC of
54 the hippocampus to the cortex at birth, allowing insight into the development of human memory
55 systems.

56

Introduction

Many adults cannot voluntarily recall memories before the ages of 3-5, a phenomenon referred to as "infantile amnesia" (Alberini & Travaglia, 2017). One potential reason for this is that the hippocampus (the primary brain structure responsible for episodic memory formation in adults) and its connections with the rest of the brain may be immature at birth. Indeed, the hippocampus does appear to be immature at birth; evidence in macaques suggests it continues to mature after one year of age (roughly age 3-5 in humans) (Jabés et al., 2011) and human data indicates that volumetric and structural changes in the hippocampus continue through childhood (DeMaster et al., 2014; Gilmore et al., 2012; Seress 2007). Further, episodic memory performance may be influenced by changes in the patterns of hippocampal connectivity from middle childhood to adulthood, including along the long-axis of the hippocampus (Blankenship et al., 2017; DeMaster et al., 2014; Ghetti et al., 2010; Gogtay et al., 2006; Poppenk & Moscovitch, 2011). However, the intrinsic connectivity of hippocampus very early in life is less well understood. Therefore, an understanding of the hippocampal network at birth and its development may lead to greater understanding of memory development.

Recently, Wael and colleagues (2018) showed the hippocampus has a clear intrinsic pattern of functional connectivity (FC) to a set of cortical networks in adults. Further, this connectivity pattern differed between the anterior and posterior portions of the hippocampus. This so-called long-axis specialization of the hippocampus is consistent with previous research showing that the anterior and posterior hippocampus display different patterns of structural and functional connectivity and may be uniquely activated in response to cognitive, memory and spatial demands (for reviews see Poppenk et al., 2013, Strange et al., 2014). The development of the hippocampal

network and the long-axis gradient likely plays a significant part in the emergence of the ability to form long-lasting memories, although little is known about it, especially in humans.

To this end, we compared the resting-state hippocampal connectivity patterns to a set of cortical networks in neonates and adults. Resting state connectivity, determined by spontaneously correlated activity of disparate brain regions, is used as a reliable marker of intrinsic functional connectivity (FC) between brain regions (Biswal et al., 1995; Raichle, 2009; Smith, 2013; Sporns, 2013); further, FC at rest is predictive of task-based activity (Cole et al., 2014; Osher et al., 2019; Smith et al., 2009; Tobyne et al., 2018).

More recently, developmental studies using FC have shown the FC of some networks is mature at birth while others take months or longer to become adultlike (for reviews see Gao et al., 2017 and Grayson & Fair, 2017). In particular, multiple studies indicate that the connectivity of visual and somatomotor networks are functional at birth (Gao et al., 2015b; Lin et al., 2008; Liu et al., 2008) while other areas such as the default mode network, dorsal attention network and frontoparietal networks continue to develop postnatally (Gao et al., 2015b).

To assess hippocampal maturity at birth, we analyzed FC between seven intrinsic networks and the hippocampus as a whole as well as along the hippocampal long-axis in both neonates and adults. We also compared neonatal vs. adult hippocampal connectivity to the cortex at a finer, voxelwise scale. Based on previous literature suggesting the immaturity of the hippocampus at birth, we expected to see differences between adults and neonates in their hippocampal connectivity to the cortex, particularly to the more immature networks (e.g. default mode and frontoparietal).

Materials and Methods

Participants

Neonates:

Neonatal data comes from the initial release of the Developing Human Connectome Project (dHCP) (http://www.developingconnectome.org, Markopoulos et al., 2018). Neonates were recruited and imaged in London at the Evelina Neonatal Imaging Centre after gathering informed parental consent to image and release the data. The study was approved by the UK Health Research Authority. 40 neonates were included in our analyses (15 female, 36-44 weeks old at scan).

Adults:

Adult data comes from the Human Connectome Project (HCP), WU-Minn HCP 1200 Subject Data Release (https://www.humanconnectome.org/study/hcp-young-adult, Van Essen et al., 2013). Participants were scanned at Washington University in St. Louis (WashU). We included 40 participants in our analyses (15 female; 20-35 years old). These adult participants were motion-matched to the neonates. Specifically, we matched each neonatal participant with an adult from the HCP dataset with the same gender who showed the most similar motion parameter (i.e., framewise displacement, FD) with the *k*-nearest neighbors' approach.

MRI Acquisition

Neonates:

All acquisition information comes from the dHCP data release documentation. Imaging was carried out on a 3T Philips Achieva (running modified R3.2.2 software) using an imaging system specifically designed for neonates with a 32 channel phased array head coil (Hughes, E.J., et al.). Neonates were scanned during natural sleep; resting-state FC patterns have been shown to

stay largely consistent while awake, asleep, or under anesthesia (Liu et al., 2015; Larson-Prior et al., 2009).

Resting-state fMRI

High temporal resolution fMRI developed specifically for neonates was collected using multiband (MB) 9x accelerated echo=planar imaging (TE/TR=38/392ms, voxel size = 2.15 x 2.15 x 2.15mm^3). The resting state scan lasted approximately 15 minutes and consisted of 2300 volumes for each run. No in-plane acceleration or partial Fourier transform was used. Single-band reference scans with bandwidth matched readout and additional spin-echo acquisitions were also acquired with both AP/PA fold-over encoded directions.

Anatomical MRI

High-resolution T2-weighted and inversion recovery T1-weighted multi-slice fast spin-echo images were acquired with in-plane resolution 0.8 x 0.8mm^2 and 1.6mm slices overlapped by 0.8mm (T2-weighted: TE/TR= 156/12000ms; T1 weighted: TE/TR/TI = 8.7/4795/1740ms)

<u>Adults:</u>

All acquisition information comes from the HCP data release documentation. Scanning for the 1200 WU-Minn HCP subject was carried out on a customized 3T Connectome Scanner adapted from a Siemens Skyra (Siemens AG, Erlanger, Germany), equipped with a 32-channel Siemens receiver head coil and a “body” transmission coil specifically designed by Siemens to accommodate the smaller space (due to special gradients) of the WU-Minn and MGH-UCLA Connectome scanners.

148

149 *Resting-State fMRI*

150 Participants were scanned using the Gradient-echo EPI sequence (TE/TR = 33.1/720ms,
151 flip angle = 52°, 72 slices, voxel size = 2 x 2 x 2mm^{3}). Scanning lasted approximately 15 minutes
152 consisting of 1200 volumes for each run. Each participant finished two resting-state fMRI sessions.
153 For each session, two phases were encoded: one right-to-left (RL) and the other left-to-right (LR).
154 For our analyses, we used the LR phase encoding from the first session. Participants were
155 instructed to relax and keep their eyes open and fixated on a bright, projected cross-hair against a
156 dark background.

157

158 *Anatomical MRI*

159 High-resolution T2-weighted and T1-weighted images were acquired with an isotropic
160 voxel resolution of 0.7mm^{3} (T2-weighted 3D T2-SPACE scan: TE/TR=565/3200ms; T1-weighted
161 3D MPRAGE: TE/TR/TI = 2.14/2400/1000ms).

162

163 **MRI Preprocessing**

164 Neonates:

165 The dHCP data was preprocessed using the dHCP minimal preprocessing pipelines
166 (Makropoulos et al., 2018). Anatomical MRI preprocessing included bias correction, brain
167 extraction using BET from FSL (FMRIB Software Library) and segmentation of the T2w volume
168 using their DRAW-EM algorithm (Makropoulos et al., 2014). The resulted gray and white matter
169 segmentations were used as anatomical masks in further analyses; these masks were manually
170 checked for accuracy.

171 Minimal preprocessing for the resting-state fMRI included (Fitzgibbon et al., 2016)
172 distortion correction, motion correction, 2-stage registration of the MB-EPI functional image to
173 the T2 structural image, temporal high-pass filtering (150s high-pass cutoff), and ICA denoising
174 using FSL's FIX (Salimi-Khorshidi, et al., 2014). In addition to this minimal preprocessing, we
175 smoothed the data (Gaussian filter, FWHM = 3mm) across the gray matter, and applied a band-
176 pass filter at 0.009-0.08 Hz. To further denoise the data, we used aCompCor (Behzadi et al., 2007)
177 to regress out physiological noise (heartbeat, respiration, etc.) from the white matter and
178 cerebrospinal fluid (CSF).

179 Adults:

180 HCP data was preprocessed using the HCP minimal preprocessing pipelines (Glasser et al.,
181 2013). For the anatomical data, a Pre-FreeSurfer pipeline was applied to correct gradient distortion,
182 produce an undistorted "native" structural volume space for each adult participant by ACPC
183 registration (hereafter referred to as "acpc space"), extract the brain, perform a bias field
184 correction, and register the T2-weighted image to the T1-weighted image. Additionally, each
185 participant's brain was aligned to a common MNI152 template brain (with 0.7mm isotropic
186 resolution). Then, the FreeSurfer pipeline (based on FreeSurfer 5.3.0-HCP) was performed with a
187 number of enhancements specifically designed to capitalize on HCP data (Glasser et al., 2013).
188 The goal of this pipeline was to segment the volume into predefined structures, to reconstruct the
189 white and pial cortical surfaces, and to perform FreeSurfer's standard folding-based surface
190 registration to their surface atlas (fsaverage).

191 For the resting-state fMRI data, minimal functional analysis pipelines included: removing
192 spatial distortions, motion correction, registering the fMRI data to structural and MNI152
193 templates, reducing the bias field, normalizing the 4D image to a global mean, and masking the

194 data with the final brain mask. After completing these steps, the data were further denoised using
195 the ICA-FIX method (Salimi-Khorshidi, et al., 2014). To mirror the adult and neonatal
196 preprocessing pipelines, we unwarped the data from MNI152 to acpc space, allowing both groups
197 to be analyzed in "native" space. We then applied spatial smoothing (Gaussian filter, FWHM =
198 3mm) within the gray matter, band-pass filtered at 0.009-0.08 Hz and implemented aCompCor to
199 regress out physiological noise, just as we did with the neonates.

200 All subsequent analyses in neonates and adults were performed in each subject's native
201 space, except for the whole-brain voxelwise analysis.

202 **Connectivity analyses**

203 We used the 7-network cortical parcellation identified by Yeo et al. (2011). For the
204 whole-hippocampus and long-axis analyses, the hippocampal label was binarized from
205 FreeSurfer's (surfer.nmr.mgh.harvard.edu) aparc+aseg parcellation and visually inspected for
206 accuracy in each subject. For the first long-axis gradient analysis this label was further sectioned
207 into anterior and posterior portions via manual segmentation using FreeSurfer, with the uncal
208 apex as the dividing marker (Poppenk & Moscovitch., 2011). All labels (cortical networks,
209 hippocampal labels) were originally in CVS average-35 MNI152 space and then registered to
210 each individual subject's anatomical data using ANTs (Advanced Normalization Tool)
211 3dWarpMultiTransform (ANTs version 2.1.0; http://stnava.github.io/ANTs; Avants et al., 2011)
212). ANTs is routinely used for developmental dataset registrations (Alexander et al., 2019; Dean et
213 al., 2018). The resulting registrations were checked for accuracy. Similarly, for the long-axis
214 gradient analysis, the hippocampal label in CVS was split into nine equally spaced "slices" along
215 the anterior-posterior axis.

We then registered the labels onto the functional data in neonates using an inverse warp of the func2anat matrix provided by the dHCP. In adults, the labels in acpc space after ANTs registration were then resampled to 2mm cubic voxels to align with the functional data. We manually checked individuals from each sample to ensure the accuracy and fit of the labels to the individual functional data. We extracted the BOLD activation in each label over the time course, averaged within each label, and correlated the hippocampal activity—first whole hippocampus, then along the long-axis (for both anterior-posterior and gradient slices)—with activity in each of the 7 networks to create a Fisher's Z-scored correlation matrix using Matlab 2018b (The MathWorks, Inc., Natick, Massachusetts, United States).

We also explored differences in the hippocampal connectivity to the whole cortex at a voxelwise scale between adults and neonates to determine whether specific regions within the networks were driving adult-neonate differences. Hippocampal connectivity to the cortex was calculated by correlating the average hippocampal signal and the signal of each voxel within the cortical gray matter mask during the time course for each individual in functional space. To compare the connectivity between adults and neonates, images from both groups were registered to the template space (i.e., CVS average-35 MNI152) before running a between-group analysis. Although this is the only template-space analysis we performed, template-space analyses have been routinely performed to compare infants to adults using similar registration methods (e.g. Gao et al., 2009; Gao et al., 2015a).

Experimental Design and Statistical Analyses

Where t-tests were performed between regions we corrected for multiple comparisons using the Holm-Bonferroni correction (Holm, 1979); all connectivity values were Fisher's Z transformed (Fisher, 1915) to normalize the data.

239 Before doing any of the planned analyses, we first performed data quality checks. To make
240 sure there was no significant motion difference between groups, we calculated the framewise
241 displacement (FD) (Power et al., 2012) based on the six motion parameters estimated from a rigid-
242 body transformation provided by dHCP and HCP. We manually checked the registration of the
243 gray and white matter masks as well as the network and hippocampal labels in the adults and
244 neonates to the registration was accurate. Because we are performing comparisons of correlations
245 between groups, we next wanted to ensure that the correlation distributions were similar and were
246 normally distributed in both neonates and adults; we did this by assessing the correlation of each
247 voxel to every other voxel in the brain and plotting the distribution of those correlations. We also
248 performed between-subject reliability of correlation matrices within and across the adult and
249 neonate groups. We calculated the connectivity of each region (i.e. each of the seven networks and
250 the hippocampus) to every other region for each subject. This connectivity matrix was then
251 correlated with every other subject's value either between- or within-groups to assess inter-subject
252 reliability; in other words, we correlated the connectivity of every adult to every other adult
253 (within-group) and neonate to neonate, as well as comparing every adult to every neonate
254 (between-group).

255 Our first analysis examined the relationship of the whole hippocampus to the seven cortical
256 networks. After running a one-way ANOVA with network as the independent variable and
257 connectivity as the dependent variable for both groups, we computed pairwise comparisons
258 between each unique combination of connectivity values to the networks (e.g. Hipp-Lim vs Hipp-
259 VA) to determine networks with significantly different FC to the hippocampus (Snedecor and
260 Cochran, 1989). Rose plots comparing the connectivity pattern of adults and neonates were created
261 by subtracting the mean connectivity across all networks from each individual network (for adults

262 and neonates separately) and plotting the resulting magnitude to show the relative connectivity
263 patterns of the hippocampus to the networks for each group and to compare these patterns between
264 groups.

265 For our hippocampal-cortical voxelwise analysis, we used FSL's randomise function to
266 compare between groups and perform permutation testing (to correct for multiple comparisons) in
267 order to determine areas of greater connectivity in adults vs neonates and visa versa. After mapping
268 the individual correlation matrices from subject space into a common template space, we used
269 randomise with default 5000 permutations and clustered the results using FSL's threshold-free
270 cluster enhancement (TFCE), which corrects for family-wise error (FWE). This produced a list of
271 potential clusters with each cluster's associated p-value; the p-values were then thresholded at a
272 $p < 0.0005$, and only those clusters that remained significant after that point are reported in this
273 paper.

274 For the first long-axis hippocampus analysis, we first computed a two-way ANOVA in
275 each group (separately) using location (i.e. anterior or posterior hippocampus) and network as
276 independent variables and FC as the dependent variable. Pairwise comparisons were then made
277 between the anterior and posterior FC values to each network for each group (e.g. adult antHipp-
278 Lim vs adult postHipp-Lim). For the second long-axis analysis, we conducted a two-way ANOVA
279 at each slice using group and network as independent variables and connectivity as the dependent
280 variable. We also computed a one-way ANOVA at each slice for each group with network as the
281 independent variable. As in the whole-hippocampal analysis, rose plots were created by
282 subtracting out the mean connectivity to all networks (e.g. mean connectivity of adult anterior
283 hippocampus to all networks) from each network and group in the anterior and posterior labels

284 individually to demonstrate comparative connectivity differences between the anterior and
285 posterior regions in each group.

286 **Results**

287 (FIGURE 1 HERE)

288 **Preliminary data-checks**

289 Comparison of the framewise displacement in adults and neonates showed no significant
290 difference of FD between adults and neonates (t(78)=-0.48, p=0.63). Visual inspection of the
291 gray and white matter masks (which are critical for resting-state preprocessing) in Figure 1a
292 shows they are accurately delineating gray/white matter in both neonates and adults; the cortical
293 networks and hippocampal labels also appear to be correctly localized, suggesting that the
294 regions are accurately identified in both neonates and adults (Figure 1a). Figure 1b demonstrates
295 that both neonates and adults have normally-distributed correlation values that are centered
296 around 0. Between-subject reliability of correlation matrices within and across the adult and
297 neonate groups showed the connectivity matrices (i.e. region-to-region connectivity of each of
298 the seven networks and the hippocampus to each other) of each adult subject to each other adult
299 subject were highly correlated, as were the matrices of each neonate subject to each other
300 neonate subject, and a pairwise comparison of subject variability within groups (e.g. adult-adult
301 correlations compared to neonate-neonate correlations) was not significant (t(78)=0.76, p=0.45).
302 But subject-to-subject correlations across the two groups were significantly lower than the
303 within-group correlations (adult-adult vs adult-neo t(78) = 14.09, $p=3.87x10^{-23}$, neonate-neonate
304 vs adult-neonate (t(78)=11.95, $p=2.63x10^{-19}$) suggesting that while the connectivity data are
305 reliable, neonates have different connectivity patterns than adults.

306 **Whole Hippocampus**

We first explored the connectivity of the whole hippocampus to the cortical networks. In adults, there was a main effect of network suggesting that some networks are more strongly connected with the hippocampus than others (Figure 2; one-way ANOVA, $F(6,273)=47.11$, $p=1.84\times10^{-39}$). Subsequent pairwise comparisons showed a clear hierarchy of connectivity, such that hippocampal connectivity was highest to the Limbic (Lim) network (vs hippocampal connectivity to: Ventral Attention or VA ($t(78)=12.95$, $p_{HB}=8.42\times10^{-20}$); FrontoParietal or FP ($t(78)=11.76$, $p_{HB}=1.20\times10^{-17}$), Dorsal Attention or DA ($t(78)=10.09$, $p_{HB}=1.50\times10^{-14}$);Visual or Vis ($t(78)=7.20$, $p_{HB}=4.52\times10^{-9}$); and SomatoMotor or SM ($t(78)=5.97$, $p_{HB}=7.91\times10^{-7}$)). Hippocampal connectivity to the Default Mode Network (DM) was higher than hippocampal connectivity to: VA ($t(78)=10.32$, $p_{HB}=5.80\times10^{-15}$); FP ($t(78)=9.07$, $p_{HB}=1.33\times10^{-12}$); DA ($t(78)=7.24$, $p_{HB}=4.04\times10^{-9}$); Vis ($t(78)=4.63$, $p_{HB}=1.45\times10^{-4}$); and SM ($t(78)=3.16$, $p_{HB}=0.014$)). Hippocampal-SM connectivity was 3rd highest, and higher than hippocampal connectivity to: VA ($t(78)=7.83$, $p_{HB}=3.19\times10^{-10}$); FP ($t(78)=6.46$, $p_{HB}=1.09\times10^{-7}$); and DA ($t(78)=4.35$, $p_{HB}=3.61\times10^{-4}$)). Hippocampal-Vis connectivity was the next highest (vs VA ($t(78)=5.49$, $p_{HB}=5.31\times10^{-6}$); FP ($t(78)=4.16$, $p_{HB}=6.38\times10^{-4}$), and connectivity with DA was higher than with VA ($t(78)=3.89$, $p_{HB}=1.47\times10^{-3}$). In summary, hippocampal connectivity was highest to Lim, followed by DM, then SM, Vis, and DA; hippocampal connectivity was lowest (i.e. negatively correlated) with the FP and VA networks. In previous literature, the hippocampus is occasionally included as a part of the DM network; our finding of high Hippocampal-DM correlation and anti-correlation between the hippocampus and attention (i.e. FP and VA) networks falls in line with earlier work on the connectivity of the DM network (e.g. Buckner, Andrews-Hanna & Schacter, 2008) and is a good sign of the reliability of our results.

In contrast to the adult pattern, although neonates did show a main effect of network ($F(6,273)=5.12$, $p=2.27x10^{-5}$), pairwise comparisons indicated that only the Lim and SM networks significantly differ from the rest, with significantly greater connectivity from the hippocampus to Lim vs DA (($t(78)=5.31$, $p_{HB}=2.15x10^{-5}$) and Lim vs FP ($t(78)=4.22$, $p_{HB}=1.33x10^{-3}$) and significantly greater connectivity to SM vs DA($t(78)=3.35$, $p_{HB}=0.023$).

Pairwise comparisons between adults and neonates showed significant differences between the groups, with significantly less connectivity in adults to Vis ($t(78)=-2.64$, $p_{HB}=0.040$), DA($t(78) =-2.77$, $p_{HB}=0.035$), FP($t(78)=-5.33$, $p_{HB}=5.49x10^{-6}$) and VA ($t(78)=-8.62$, $p_{HB}=5.86x10^{-13}$) networks compared to neonates.

(FIGURE 2 HERE)**Hippocampus to Cortex voxelwise analysis**

We next explored the connectivity of the hippocampus to the entire cortex at a voxelwise scale; because our previous analysis only focused on 7 canonical networks, we may have missed differences between neonates and adults at a finer grain than that seen on a network level. Thresholding the unpaired t-test results of the whole-brain clusters at $p<0.0005$ produced 26 significant FWE-corrected (Smith & Nichols, 2009) clusters in the neonates > adults comparison (i.e. 26 clusters where neonatal hippocampal FC significantly exceeds adult hippocampal FC) and 14 significant clusters in the adults > neonates comparison (Figure 3). Specifically, neonates show greater hippocampal FC to frontal and parietal areas, bilateral lingual and pericalcarine cortex and cuneus when compared to adults; frontoparietal differences were particularly prevalent within the right hemisphere. Adults, on the other hand, displayed greater hippocampal FC than the neonates primarily to bilateral isthmus cingulate and precuneus. Cluster sizes and indices for clusters greater than 200 voxels along with peak voxel location and associated brain regions are reported in Figures 3-1 and 3-2 and largely follow the results from the 7-network

analysis—the neonatal hippocampus shows greater FC to frontoparietal and attention-relevant areas, whereas the adult hippocampus shows greater FC with regions associated with the default mode and limbic networks.

(FIGURE 3 HERE)

Anterior-Posterior Hippocampus

We next explored the anterior vs. posterior hippocampal connectivity patterns in neonates and adults; previous literature in both humans and other animals suggest functional differentiation of the anterior and posterior hippocampal segments, and thus we may expect these segments to have differences in FC to the 7 cortical networks. In adults, a two-way ANOVA indicated a main effect of network ($F(6,546)=60.04.$, $p=5.04x10^{-57}$) and an interaction between network and anterior/poster hippocampus ($F(6,546)=14.31$, $p=3.54x10^{-15}$) (Figure 4). In neonates, the two-way ANOVA showed only a significant main effect for network ($f(6,546)=7.67$, $p=6.30x10^{-8}$) (Figure 4). Pairwise comparisons between the anterior and posterior portions of the hippocampus in adults show greater anterior vs posterior connectivity to the Lim ($t(78)=3.53$, $p_{HB}=0.0035$), DMN ($t(78)=2.38$, $p_{HB}=0.03$) and SM ($t(78)=3.19$, $p_{HB}=0.0082$) networks, and decreased anterior vs posterior connectivity to the DA ($t(78)=-3.07$, $p_{HB}=0.0087$), Frontoparietal ($t(78)=-5.79$, $p_{HB}=9.99x10^{-7}$) and VA ($t(78)=-3.92$, $p_{HB}=0.0011$) networks. These results suggest the anterior hippocampus was primarily driving the negative correlations with VA & FP seen at the level of the whole hippocampus in adults. Neonates, however, show no significant differences between the anterior and posterior portions of the hippocampus to any of the networks, suggesting no differentiation/specialization of the hippocampal segments in their connections to the rest of the brain.

(FIGURE 4 HERE)

Long-Axis Gradient

Finally, we investigated the long-axis gradient, which has been demonstrated to map onto a differential functional gradient of the hippocampus. We broke up the hippocampus in each subject into 9 different segments along the anterior-posterior axis and compared the 7-network connectivity to these segments in neonates and adults. Adults showed clear differentiation of network connectivity along the long-axis while neonates showed no clear differentiation (Figure 5). The Lim and DM in adults appeared to have an initial rise and fall of FC along the anterior-posterior gradient of the hippocampus which differentiated them from the Vis, SM, and DA, and the FP and VA showed a similar rise and fall of negative FC along the gradient. One-way ANOVAs for adults and neonates at each slice indicated a main effect of network in adults in all but the most posterior slice (Slice 1 ($F(6,273)=23.61$, $p=1.89\times10^{-22}$), Slice 2 ($F(6,273)=40.45$, $p=4.19\times10^{-35}$), Slice 3 ($F(6,273)=50.09$, $p=2.61\times10^{-41}$), Slice 4 ($F(6,273)=49.56$, $p=5.48\times10^{-41}$), Slice 5 ($F(6,273)=49.07$, $p=1.11\times10^{-40}$), Slice 6 ($F(6,273)=25.10$, $p=1.12\times10^{-23}$), Slice 7 ($F(6,273)=13.40$, $p=2.57\times10^{-13}$), Slice 8 ($F(6,273)=5.51$, $p=2.12\times10^{-5}$)). In the neonates, there was no main effect of network in any of the slices (at $p<0.001$). To compare between the two groups, we performed two-way ANOVAs (with network and group as independent variables and FC value as the dependent variable) for each of the 9 slices. There was a significant interaction between network and group for the anterior 7 slices (Slice 1 ($F(6,546)=7.30$, $p=1.64\times10^{-7}$), Slice 2 ($F(6,546)=16.25$, $p=2.95\times10^{-17}$), Slice 3 ($F(6,546)=18.98$, $p=3.99\times10^{-20}$), Slice 4 ($F(6,546)=17.22$, $p=2.83\times10^{-18}$), Slice 5 ($F(6,546)=17.93$, $p=5.05\times10^{-19}$), Slice 6 ($F(6,546)=5.79$, $p=7.26\times10^{-6}$), Slice 7 ($F(6,546)=4.87$, $p=7.27\times10^{-5}$) and Slice 8($F(6,546)=3.89$, $p=8.26\times10^{-4}$), but no group differences for the most posterior slice. These results show that the biggest

397 differentiation of hippocampal connectivity to the 7 networks occurs in the anterior 2/3s of the
398 hippocampus in adults and that neonates do not show this differentiation.
399 (FIGURE 5 HERE)

400 **Discussion**

401 Our results show that the intrinsic connectivity of the hippocampal network is not fully
402 mature at birth. Previous functional and volumetric evidence in both non-human primates and
403 humans suggests that the hippocampus continues to develop beyond one year of age, even into
404 middle childhood (Blankenship et al., 2017; Jabes et al., 2011; Keresztes et al., 2018; Lavenex
405 and Banta Lavenex, 2013; Riggins et al., 2016). Although there is some evidence to suggest that
406 the hippocampus is playing a key role in memory formation even early on in rodents (Alberini &
407 Travaglia, 2017; Travaglia et al., 2018), it has been suggested that the long-lasting memories of
408 very young children may be created in a fundamentally different way from adult long-term
409 memories and may rely on cortical mechanisms rather than the traditional hippocampal method
410 (Ellis & Turke-Browne, 2018; Gómez & Edgkin, 2016). Our study suggests that the
411 hippocampus does not have preferential connectivity to any particular network at birth and lacks
412 any long-axis gradient of connectivity, suggesting that the hippocampus, the cortical networks it
413 interacts with, or some combination of both, are immature at birth and may therefore be unable
414 to form long-term memories using adult-like mechanisms. Indeed, the cortex itself is still
415 maturing early on (e.g. Gao et al., 2015b; Ofen et al., 2007; Salzwedel et al., 2019) and it is
416 likely this cortical immaturity, in addition to hippocampal immaturity, is contributing to the
417 differences in memory formation between adults and neonates.

418 Adults showed a clear hierarchy of FC to the seven networks (consistent with Wael et al.
419 (2018)), whereas neonates lacked this hierarchy. Further, the comparison between adults and

420 neonates shows significant differences between groups to all networks except the SM network,
421 and only marginally significant differences between groups in the Vis and DA networks. The
422 similarity between adults and neonates in connectivity to the SM and Vis networks may be due
423 to the relative maturity of these areas at birth (Arcaro & Livingstone, 2017; Deen et al., 2017;
424 Hurk et al., 2017; Gao et al. 2017, Dall'Orso et al., 2018).

425 To more specifically determine which regions in the networks were responsible for the
426 differences seen between adults and neonates, we conducted a voxel-wise cortical analysis. Our
427 results indicate that neonates have higher connectivity to much of the cortex as compared to
428 adults with the exception of areas of bilateral medial orbitofrontal, isthmus cingulate and
429 precuneus. This is consistent with Riggins et al.'s (2016) conclusion that 4-year old children rely
430 more on regions "outside" the canonical hippocampal network to complete episodic memory
431 tasks, and other research suggesting the infant cortex is more broadly tuned than in adults (Ellis
432 &Turk-Browne, 2018). The few regions where adults display higher FC than neonates reside
433 mainly within DM network and highlight the immaturity of this network: adults show
434 significantly greater DM-Hippocampal connectivity than neonates, consistent with Gao et al.'s
435 (2015) finding that this network is one of the last to develop in the first year of life.

436 Our anterior-posterior analysis and long-axis gradient analyses again suggest that the FC
437 differentiation of the hippocampus is lacking at birth. Consistent with previous literature, adults
438 display changes along the long-axis such that the anterior hippocampus shows greater
439 connectivity to the Lim network than the posterior hippocampus but greater posterior vs anterior
440 FC to the attention (i.e. FP and VA) networks; in fact, the anterior hippocampus is especially
441 anti-correlated with these networks, as is consistent with previous literature (Buckner et al.,
442 2009; Wael et al., 2018). The greatest differentiation in FC to the networks in adults occurred

within the anterior two-thirds of the hippocampus. In contrast, neonates showed no specificity to any of the networks along the long-axis or the anterior-posterior analysis. Blankenship et al. (2017), Langnes et al. (2018), and Riggins et al. (2016) show evidence of specialization along the longitudinal axis in 4- and 6-year old children but no such evidence is seen in our results, suggesting that maturational changes within the hippocampus may occur before age 4 to produce the preferential connectivity seen in children and adults. Future studies of infants and toddlers can better elucidate when after birth this change in specialization of the long-axis occurs.

Several limitations warrant discussion. A major problem in imaging children is motion artifact. We used the motion-corrected data that were released by the dHCP, took steps in preprocessing to ensure that physiological artifacts were removed from the data in both neonates and adults (Power et al., 2014; Yan et al., 2013), and further motion-matched the neonatal and adult groups. Given that motion-related artifacts are a major confound in FC analyses (Power et al., 2012; Satterthwaite et al., 2013), our approach should minimize the risk of spurious correlations. Other steps we took to minimize potential confounds included visual inspection of spatial registration results (and using established registration procedures that have been previously performed on infants (Alexander et al., 2019; Dean et al., 2018; Gao et al., 2009; Gao et al., 2015a)), performing the analyses in the native-space of each individual, and checking the reliability of the correlation values across participants in each group to ensure they were not particularly noisy in the neonatal group. A result of particular note is that neonates showed primarily positive FC from the hippocampus to the networks, while adults showed slightly negative FC for some networks. Blankenship et al., (2017) similarly fail to show any negative hippocampal FC in their sample of 4- and 6-year old children (but this may be due to their preprocessing steps, see Murphy & Fox, 2017 for discussion). Here, we used the same

466 preprocessing steps in both neonates and adults and used aCompCor and other preprocessing
467 steps that should not necessarily remove negative correlations if they were there. Indeed, we
468 found a normal distribution of correlation values in both neonates and adults (Figure 1)
469 suggesting that negative correlations do exist in neonates, but not between the hippocampus and
470 the cortex. Further, regardless of the negative vs. positive correlation differences we observe a
471 difference in the pattern of FC in adults (demonstrated in the rose plots) primarily in the anterior
472 portion of the hippocampus; this is missing in neonates.

473 In conclusion, our results suggest that the resting-state FC patterns of the human
474 hippocampus are immature at birth. This immaturity may play a key role in infantile amnesia and
475 the vast differences between adults and neonates shown here suggests a fundamentally different
476 memory and learning system from that of adults may be present at this point in development.

477 **References**

478 Alberini, C. M., & Travaglia, A. (2017). Infantile Amnesia: A Critical Period of Learning to
479 Learn and Remember. *Journal of Neuroscience*, *37*(24), 5783–5795.

480 Alexander, B., Kelly, C. E., Adamson, C., Beare, R., Zannino, D., Chen, J., … Thompson, D. K.
481 (2019). Changes in neonatal regional brain volume associated with preterm birth and
482 perinatal factors. *NeuroImage*, *185*, 654–663.

483 Arcaro, M. J., & Livingstone, M. S. (2017). A hierarchical, retinotopic proto-organization of the
484 primate visual system at birth. *ELife*, *6*.

485 Avants, B. B., Tustison, N. J., Song, G., Cook, P. A., Klein, A., & Gee, J. C. (2011). A
486 Reproducible Evaluation of ANTs Similarity Metric Performance in Brain Image
487 Registration. *NeuroImage*, *54*(3), 2033–2044.

Behzadi, Y., Restom, K., Liau, J. & Liu, T.T.J.N. A component based noise correction method (CompCor) for BOLD and perfusion based fMRI. *Neuroimage, 37*, 90-101 (2007)

Biswal, B., Yetkin, F. Z., Haughton, V. M., & Hyde, J. S. (1995). Functional connectivity in the motor cortex of resting human brain using echo-planar mri. *Magnetic Resonance in Medicine*, *34*(4), 537–541.

Blankenship, S. L., Redcay, E., Dougherty, L. R., & Riggins, T. (2017). Development of hippocampal functional connectivity during childhood. *Human Brain Mapping*, *38*(1), 182–201.

Buckner, R. L., Andrews‐Hanna, J. R., & Schacter, D. L. (2008). The Brain’s Default Network. *Annals of the New York Academy of Sciences*, 1124(1), 1–38.

Buckner, R. L., Sepulcre, J., Talukdar, T., Krienen, F., Liu, H., Hedden, T., … Johnson, K. A. (2009). Cortical Hubs Revealed by Intrinsic Functional Connectivity: Mapping, Assessment of Stability, and Relation to Alzheimer’s Disease. *The Journal of Neuroscience : The Official Journal of the Society for Neuroscience*, *29*(6), 1860–1873.

Cole, M. W., Bassett, D. S., Power, J. D., Braver, T. S., & Petersen, S. E. (2014). Intrinsic and task-evoked network architectures of the human brain. *Neuron*, *83*(1), 238–251.

Dall’Orso, S., Steinweg, J., Allievi, A. G., Edwards, A. D., Burdet, E., & Arichi, T. (2018). Somatotopic Mapping of the Developing Sensorimotor Cortex in the Preterm Human Brain. *Cerebral Cortex*, *28*(7), 2507–2515.

Dean, D. C., Planalp, E. M., Wooten, W., Schmidt, C. K., Kecskemeti, S. R., Frye, C., … Davidson, R. J. (2018). Investigation of brain structure in the 1-month infant. *Brain Structure and Function*, *223*(4), 1953–1970.

Deen, B., Richardson, H., Dilks, D. D., Takahashi, A., Keil, B., Wald, L. L., … Saxe, R. (2017). Organization of high-level visual cortex in human infants. *Nature Communications*, *8*, 13995.

DeMaster, D., Pathman, T., Lee, J. K., & Ghetti, S. (2014). Structural development of the hippocampus and episodic memory: Developmental differences along the anterior/posterior axis. *Cerebral Cortex (New York, N.Y.: 1991)*, *24*(11), 3036–3045.

Ellis, C. T., & Turk-Browne, N. B. (2018). Infant fMRI: A Model System for Cognitive Neuroscience. *Trends in Cognitive Sciences*, *22*(5), 375–387.

Fisher, R. A. (1915). Frequency Distribution of the Values of the Correlation Coefficient in Samples from an Indefinitely Large Population. *Biometrika*, *10*(4), 507.

Fitzgibbon, S.P., et al. The developing Human Connectome Project (dHCP): minimal 406 functional pre-processing pipeline for neonates. *in Fifth Biennial Conference on Resting State and Brain Connectivity* (2016)

Gao, W., Alcauter, S., Elton, A., Hernandez-Castillo, C. R., Smith, J. K., Ramirez, J., & Lin, W. (2015). Functional Network Development During the First Year: Relative Sequence and Socioeconomic Correlations. *Cerebral Cortex (New York, NY)*, *25*(9), 2919–2928.

Gao, W., Alcauter, S., Smith, J. K., Gilmore, J., & Lin, W. (2015). Development of Human Brain Cortical Network Architecture during Infancy. *Brain Structure & Function*, *220*(2), 1173–1186.

Gao, W., Lin, W., Grewen, K., & Gilmore, J. H. (2017). Functional Connectivity of the Infant Human Brain: Plastic and Modifiable. *The Neuroscientist*, *23*(2), 169–184.

Gao, W., Zhu, H., Giovanello, K. S., Smith, J. K., Shen, D., Gilmore, J. H., & Lin, W. (2009). Evidence on the emergence of the brain's default network from 2-week-old to 2-year-old

healthy pediatric subjects. *Proceedings of the National Academy of Sciences*, *106*(16), 6790–6795.

Ghetti, S., DeMaster, D. M., Yonelinas, A. P., & Bunge, S. A. (2010). Developmental Differences in Medial Temporal Lobe Function during Memory Encoding. *Journal of Neuroscience*, *30*(28), 9548–9556.

Gilmore, J. H., Shi, F., Woolson, S. L., Knickmeyer, R. C., Short, S. J., Lin, W., … Shen, D. (2012). Longitudinal Development of Cortical and Subcortical Gray Matter from Birth to 2 Years. *Cerebral Cortex*, *22*(11), 2478–2485.

Glasser, M.F., et al. The minimal preprocessing pipelines for the Human Connectome Project. *Neuroimage*, *80*, 105-124 (2013)

Gómez, R. L., & Edgin, J. O. (2016). The extended trajectory of hippocampal development: Implications for early memory development and disorder. *Developmental Cognitive Neuroscience*, *18*, 57–69.

Gogtay, N., Nugent, T. F., Herman, D. H., Ordonez, A., Greenstein, D., Hayashi, K. M., … Thompson, P. M. (2006). Dynamic mapping of normal human hippocampal development. *Hippocampus*, *16*(8), 664–672.

Grayson, D. S., & Fair, D. A. (2017). Development of large-scale functional networks from birth to adulthood: A guide to the neuroimaging literature. *NeuroImage*, *160*, 15–31.

Holm, S. (1979). A simple sequentially rejective multiple test procedure. Scandinavian Journal of Statistics, 6, 65–70

Hughes, E.J., et al. A dedicated neonatal brain imaging system. *Magn Reson Med*. *78*, 794-804 (2017).

Hurk, J. van den, Baelen, M. V., & Beeck, H. P. O. de. (2017). Development of visual category selectivity in ventral visual cortex does not require visual experience. *Proceedings of the National Academy of Sciences*, *114*(22), E4501–E4510.

Jabès, A., Lavenex, P. B., Amaral, D. G., & Lavenex, P. (2011). Postnatal development of the hippocampal formation: A stereological study in macaque monkeys. *The Journal of Comparative Neurology*, *519*(6), 1051–1070.

Jenkinson, M., Beckmann, C. F., Behrens, T. E. J., Woolrich, M. W., & Smith, S. M. (2012). FSL. *NeuroImage*, *62(2)*, 782-790.

Keresztes, A., Ngo, C. T., Lindenberger, U., Werkle-Bergner, M., & Newcombe, N. S. (2018). Hippocampal Maturation Drives Memory from Generalization to Specificity. *Trends in Cognitive Sciences*, *22*(8), 676–686.

Langnes, E., Vidal-Piñeiro, D., Sneve, M. H., Amlien, I. K., Walhovd, K. B., & Fjell, A. M. (2018). Development and Decline of the Hippocampal Long-Axis Specialization and Differentiation During Encoding and Retrieval of Episodic Memories. *Cerebral Cortex*, *29*(8), 3398–3414.

Larson-Prior, L. J., Zempel, J. M., Nolan, T. S., Prior, F. W., Snyder, A. Z., & Raichle, M. E. (2009). Cortical network functional connectivity in the descent to sleep. *Proceedings of the National Academy of Sciences*, *106*(11), 4489–4494.

Lavenex, P., & Banta Lavenex, P. (2013). Building hippocampal circuits to learn and remember: Insights into the development of human memory. *Behavioural Brain Research*, *254*, 8–21.

Lin, W., Zhu, Q., Gao, W., Chen, Y., Toh, C.-H., Styner, M., … Gilmore, J. H. (2008). Functional Connectivity MR Imaging Reveals Cortical Functional Connectivity in the Developing Brain. *American Journal of Neuroradiology*, *29*(10), 1883–1889.

Liu, W.-C., Flax, J. F., Guise, K. G., Sukul, V., & Benasich, A. A. (2008). Functional connectivity of the sensorimotor area in naturally sleeping infants. *Brain Research*, *1223*, 42–49.

Liu, X., Yanagawa, T., Leopold, D. A., Fujii, N., & Duyn, J. H. (2015). Robust Long-Range Coordination of Spontaneous Neural Activity in Waking, Sleep and Anesthesia. *Cerebral Cortex*, *25*(9), 2929–2938.

Makropoulos, A., et al. Automatic whole brain MRI segmentation of the developing neonatal brain. *IEEE Transactions on Medical Imaging, 33*, 1818-1831 (2014).

Makropoulos, A., et al. The developing human connectome project: A minimal processing pipeline for neonatal cortical surface reconstruction. *Neuroimage*, *173*, 88-112 (2018).

Murphy, K., & Fox, M. D. (2017). Towards a consensus regarding global signal regression for resting state functional connectivity MRI. *NeuroImage*, *154*, 169–173.

Ofen, N., Kao, Y.-C., Sokol-Hessner, P., Kim, H., Whitfield-Gabrieli, S., & Gabrieli, J. D. E. (2007). Development of the declarative memory system in the human brain. *Nature Neuroscience*, *10*, 1198.

Osher, D. E., Brissenden, J. A., & Somers, D. C. (2019). Predicting an individual's dorsal attention network activity from functional connectivity fingerprints. *Journal of Neurophysiology*, *122*(1), 232–240.

Poppenk, J., Evensmoen, H. R., Moscovitch, M., & Nadel, L. (2013). Long-axis specialization of the human hippocampus. *Trends in Cognitive Sciences*, *17*(5), 230–240.

Poppenk, J., & Moscovitch, M. (2011). A Hippocampal Marker of Recollection Memory Ability among Healthy Young Adults: Contributions of Posterior and Anterior Segments. *Neuron*, *72*(6), 931–937.

Power, J. D., Barnes, K. A., Snyder, A. Z., Schlaggar, B. L., & Petersen, S. E. (2012). Spurious but systematic correlations in functional connectivity MRI networks arise from subject motion. *NeuroImage*, *59*(3), 2142–2154.

Power, J. D., Mitra, A., Laumann, T. O., Snyder, A. Z., Schlaggar, B. L., & Petersen, S. E. (2014). Methods to detect, characterize, and remove motion artifact in resting state fMRI. *NeuroImage*, *84*, 320–341.

Raichle, M. E. (2009). A Paradigm Shift in Functional Brain Imaging. *Journal of Neuroscience*, *29*(41), 12729–12734.

Riggins, T., Geng, F., Blankenship, S. L., & Redcay, E. (2016). Hippocampal functional connectivity and episodic memory in early childhood. *Developmental Cognitive Neuroscience*, *19*, 58–69

Salimi-Khorshidi, G., et al. Automatic denoising of functional MRI data: combining 409 independent component analysis and hierarchical fusion of classifiers. *Neuroimage*, *90,* 449-468 (2014)

Salzwedel, A. P., Stephens, R. L., Goldman, B. D., Lin, W., Gilmore, J. H., & Gao, W. (2019). Development of Amygdala Functional Connectivity During Infancy and Its Relationship With 4-Year Behavioral Outcomes. *Biological Psychiatry: Cognitive Neuroscience and Neuroimaging*, *4*(1), 62–71.

Satterthwaite, T. D., Elliott, M. A., Gerraty, R. T., Ruparel, K., Loughead, J., Calkins, M. E., … Wolf, D. H. (2013). An improved framework for confound regression and filtering for control of motion artifact in the preprocessing of resting-state functional connectivity data. *NeuroImage*, *64*, 240–256.

Seress, L. (2007). Comparative anatomy of the hippocampal dentate gyrus in adult and developing rodents, non-human primates and humans. In H. E. Scharfman (Ed.), *Progress in Brain Research* (pp. 23–798).

Smith, S. M., Fox, P. T., Miller, K. L., Glahn, D. C., Fox, P. M., Mackay, C. E., … Beckmann, C. F. (2009). Correspondence of the brain's functional architecture during activation and rest. *Proceedings of the National Academy of Sciences of the United States of America*, *106*(31), 13040–13045.

Smith, S. M., & Nichols, T. E. (2009). Threshold-free cluster enhancement: Addressing problems of smoothing, threshold dependence and localisation in cluster inference. *NeuroImage*, *44*(1), 83–98.

Smith, S. M., Vidaurre, D., Beckmann, C. F., Glasser, M. F., Jenkinson, M., Miller, K. L., … Van Essen, D. C. (2013). Functional connectomics from resting-state fMRI. *Trends in Cognitive Sciences*, *17*(12), 666–682.

Snedecor, GW, Cochran, WG - Ames: Iowa State Univ. Press Iowa, 1989

Sporns, O. (2013). Structure and function of complex brain networks. *Dialogues in Clinical Neuroscience*, *15*(3), 247–262.

Strange, B. A., Witter, M. P., Lein, E. S., & Moser, E. I. (2014). Functional organization of the hippocampal longitudinal axis. *Nature Reviews Neuroscience*, *15*(10), 655–669.

Thomas Yeo, B. T., Krienen, F. M., Sepulcre, J., Sabuncu, M. R., Lashkari, D., Hollinshead, M., … Buckner, R. L. (2011). The organization of the human cerebral cortex estimated by intrinsic functional connectivity. *Journal of Neurophysiology*, *106*(3), 1125–1165.

Tobyne, S. M., Somers, D. C., Brissenden, J. A., Michalka, S. W., Noyce, A. L., & Osher, D. E. (2018). Prediction of individualized task activation in sensory modality-selective frontal cortex with 'connectome fingerprinting.' *NeuroImage*, *183*, 173–185.

Travaglia, A., Steinmetz, A. B., Miranda, J. M., & Alberini, C. M. (2018). Mechanisms of critical period in the hippocampus underlie object location learning and memory in infant rats. *Learning & Memory*, *25*(4), 176–182.

Wael, R. V. de, Larivière, S., Caldairou, B., Hong, S.-J., Margulies, D. S., Jefferies, E., … Bernhardt, B. C. (2018). Anatomical and microstructural determinants of hippocampal subfield functional connectome embedding. *Proceedings of the National Academy of Sciences*, *115*(40), 10154–10159.

Wheelock, M. D., Hect, J. L., Hernandez-Andrade, E., Hassan, S. S., Romero, R., Eggebrecht, A. T., & Thomason, M. E. (2019). Sex differences in functional connectivity during fetal brain development. *Developmental Cognitive Neuroscience*, *36*, 100632.

Yan, C.-G., Cheung, B., Kelly, C., Colcombe, S., Craddock, R. C., Di Martino, A., … Milham, M. P. (2013). A comprehensive assessment of regional variation in the impact of head micromovements on functional connectomics. *NeuroImage*, *76*, 183–201.

Legends

Figure 1: Preliminary Data Checks a) Gray matter, white matter and network registrations on the anatomical images of a representative adult and neonate subject b) voxelwise correlations distributions of a representative adult and neonate c) between-subject and between-group correlations demonstrate high within-group reliability of connectivity but low between-group

reliability between adults and neonates. (*) indicates significance at $p<0.05$; ns denotes non-significance

Figure 2: Hippocampal Connectivity to Cortical Networks a) Comparison of hippocampal connectivity to the seven cortical networks in adults showed a hierarchy of hippocampal connectivity, whereby the highest FC was with Lim, followed by DM, SM, and Vis, almost no FC with DA, and negative FC with FP and VA. b) In contrast, neonates show the same level of FC to almost all of the 7 networks. Rose plot to the right shows adult connectivity compared to neonates to highlight the differences between groups in the pattern of hippocampal FC to these networks. Brain images on the top right depict connectivity between the hippocampus (left) and the seven cortical networks (right). (*) indicates significance at $p_{HB}<0.05$; (***) indicates significance at $p_{HB}<0.005$. Lim=Limbic; DM=Default Mode; SM=Somatomotor; Vis=visual; DA=Dorsal Attention; FP=FrontoParietal; VA=Ventral Attention

Figure 3: Hippocampal Connectivity to Cortex. Comparison of adult and neonate hippocampal connectivity to the cortex at a voxelwise grain. FWE-corrected results for the contrast of neonate > adult connectivity is shown in warm colors and the contrast of adult > neonate is denoted by cool colors.

Figure 4: Anterior/Posterior Hippocampal Connectivity to Networks a) Anterior vs posterior hippocampal-network connectivity in adults b) Anterior vs posterior hippocampal-network connectivity in neonates c) Rose plot comparing anterior vs posterior hippocampal-network connectivity pattern in adults d) Rose plot comparing anterior vs posterior hippocampal-network connectivity pattern in neonates. Brain image to the right shows the anterior (red) and posterior (yellow) hippocampal labels (*) indicates significance at $p_{HB}<0.05$; (***) indicates significance at $p_{HB}<0.005$.

Figure 5: Connectivity along the Long-Axis Gradient to Networks Comparison of the connectivity of the long axis gradient of the hippocampus to the 7 networks in a) adults and b) neonates. The slices are arranged anterior-to-posterior. Lighter coloring surrounding each line represents the standard error. Brain image on the right demonstrates the hippocampus (blue) segmented into slices (white lines). (*) are slices where the ANOVA shows an interaction between network and group at p<0.001.

Figures

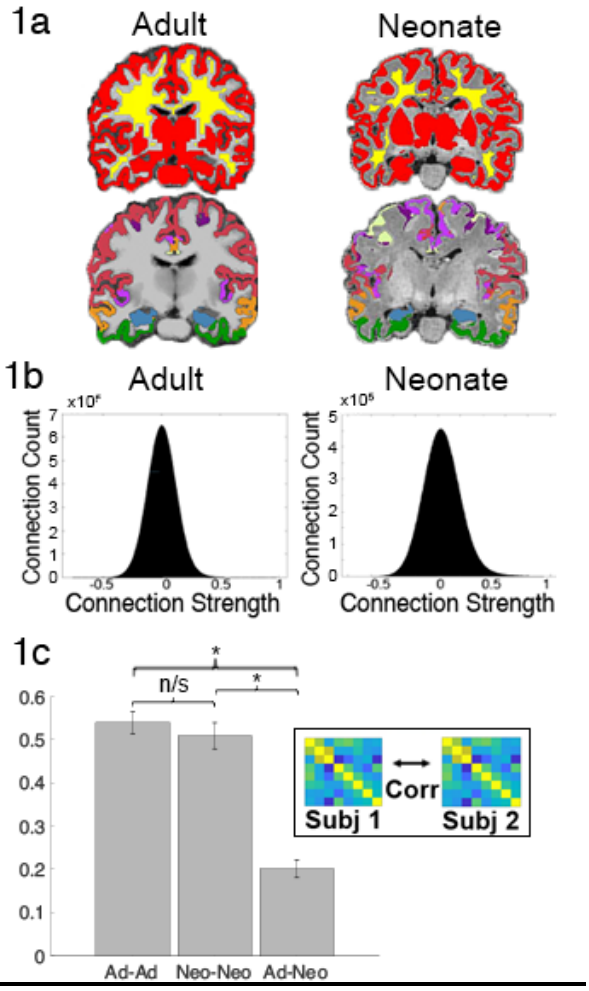

(Figure 1)

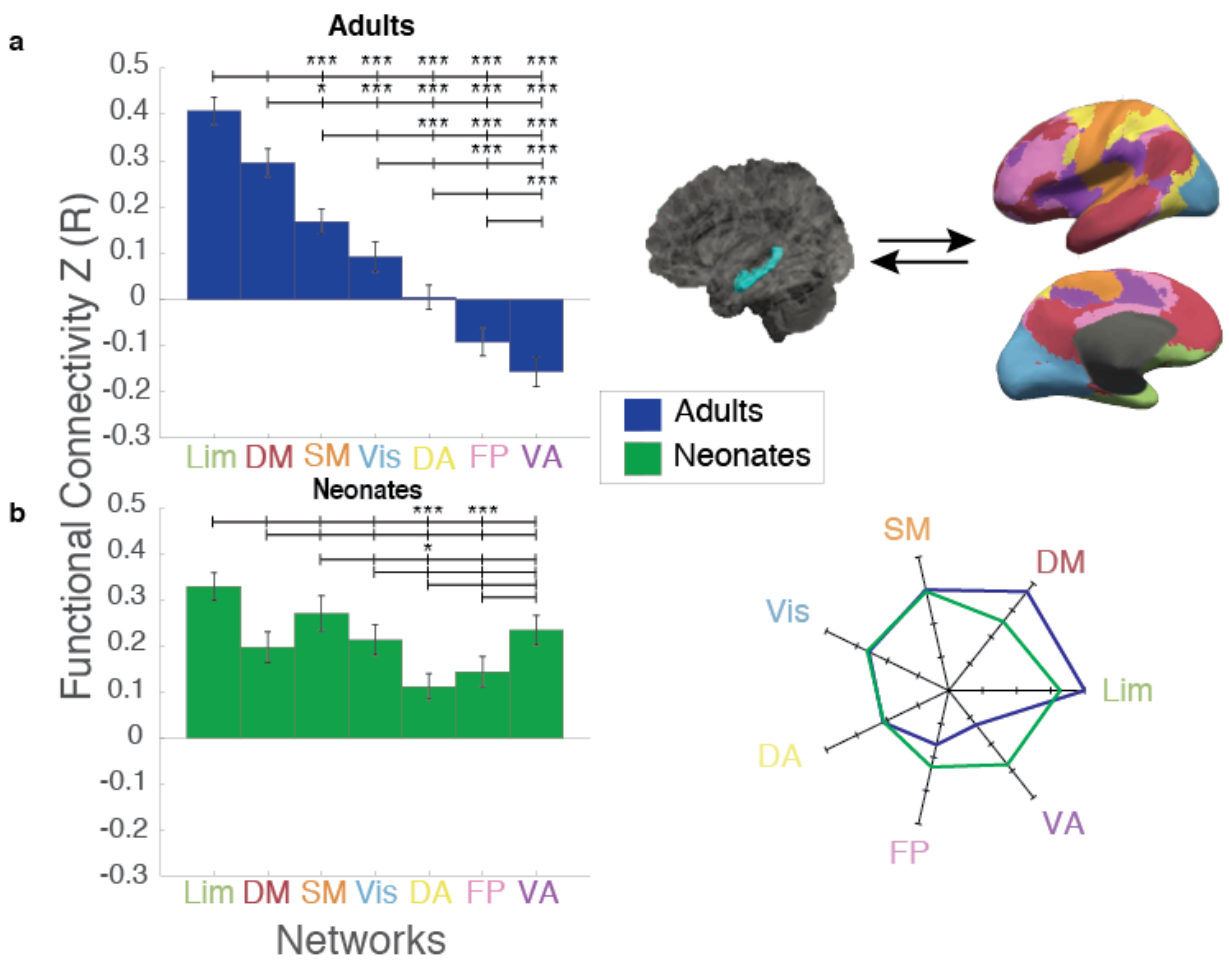
a
Adults
b
Neonates
Functional Connectivity Z (R)
0.5
0.4
0.3
0.2
0.1
0
-0.1
-0.2
-0.3
Lim DM SM Vis DA FP VA
Networks
Adults
Neonates
SM
DM
Vis
Lim
DA
VA
FP

(Figure 2)

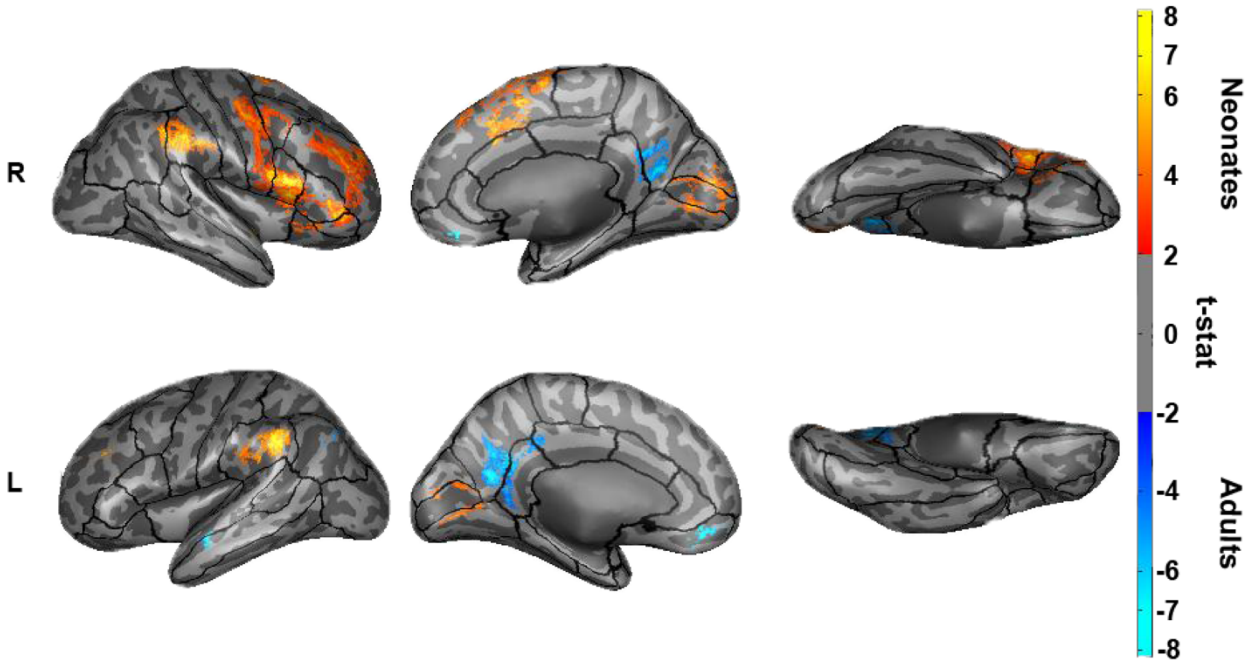

(Figure 3)

Figure 3-1: Hippocampal Connectivity to Cortex, Adult>Neo Clusters are listed from largest to smallest. Peak coordinates (MAX) are listed in MNI space as well as center of gravity (COG) for each cluster

Cluster	*Regions*	*Voxels*	*MAX*	*MAX (X)*	*MAX (Y)*	*MAX (Z)*	*COG (X)*	*COG (Y)*	*COG (Z)*
1	(L) Posterior Cingulate; Isthmus Cingulate, Precuneus	2370	8.08	-10	-57	17	-6.23	-55.2	20.8
2	(R) Isthmus Cingulate; Precuneus	1255	8.27	15	-54	19	9.3	-56.1	19.1
3	(L) Inferior Parietal	574	6.85	-42	-77	43	-44.3	-74.8	39.2
4	(L) Middle Temporal Cortex	403	5.72	-62	-1	-20	-63.2	-7.54	-18.2
5	(L) Medial Orbital Frontal	303	7.45	-10	39	-11	-7.75	41.9	-11.7
6	(L) Middle Temporal Cortex; Superior Temporal Cortex	235	6.88	-52	-13	-14	-53.1	-11.6	-13.7

Figure 3-2: Hippocampal Connectivity to Cortex, Neo>Adult Clusters are listed from largest to smallest. Peak coordinates (MAX) are listed in MNI space as well as center of gravity (COG) for each cluster

Cluster	*Regions*	*Voxels*	*MAX*	*MAX (X)*	*MAX (Y)*	*MAX (Z)*	*COG (X)*	*COG (Y)*	*COG (Z)*
1	(R) Rostral Middle Frontal; Pars Triangularis; Pars Orbitalis; Lateral Orbitofrontal; Pars Opercularis; Insula; Caudal Middle Frontal; Precentral; Postcentral	16290	8.72	57	14	4	44.9	26.2	21.8
2	(R) Superior Frontal; Paracentral	4702	6.88	4	26	61	9.85	12.7	59.4
3	(L) Supramarginal	3278	8.54	-65	-42	34	-59.6	-38.9	30.7
4	(R) Supramarginal; Inferior Parietal	3226	7.93	62	-36	48	61.8	-35.9	37.1
5	(R) Lingual; Pericalcarine (L) Lingual; Pericalcarine	2794	6.22	-19	-66	2	1.81	-77.1	5.9
6	(L) Rostral Middle Frontal	796	6.85	-34	51	29	-36.3	46.6	28.9
7	(R) Lateral Orbitofrontal; Pars Orbitalis	458	5.59	46	22	-7	39.4	24.6	-7.38
8	(L) Superior Frontal	350	5.74	-17	7	66	-13.6	8.52	69.4
9	(R) Insula	238	5.25	42	3	-6	40.4	6.44	-3.65

(Extended Data for Figure 3; Figure 3-1 and Figure 3-2)

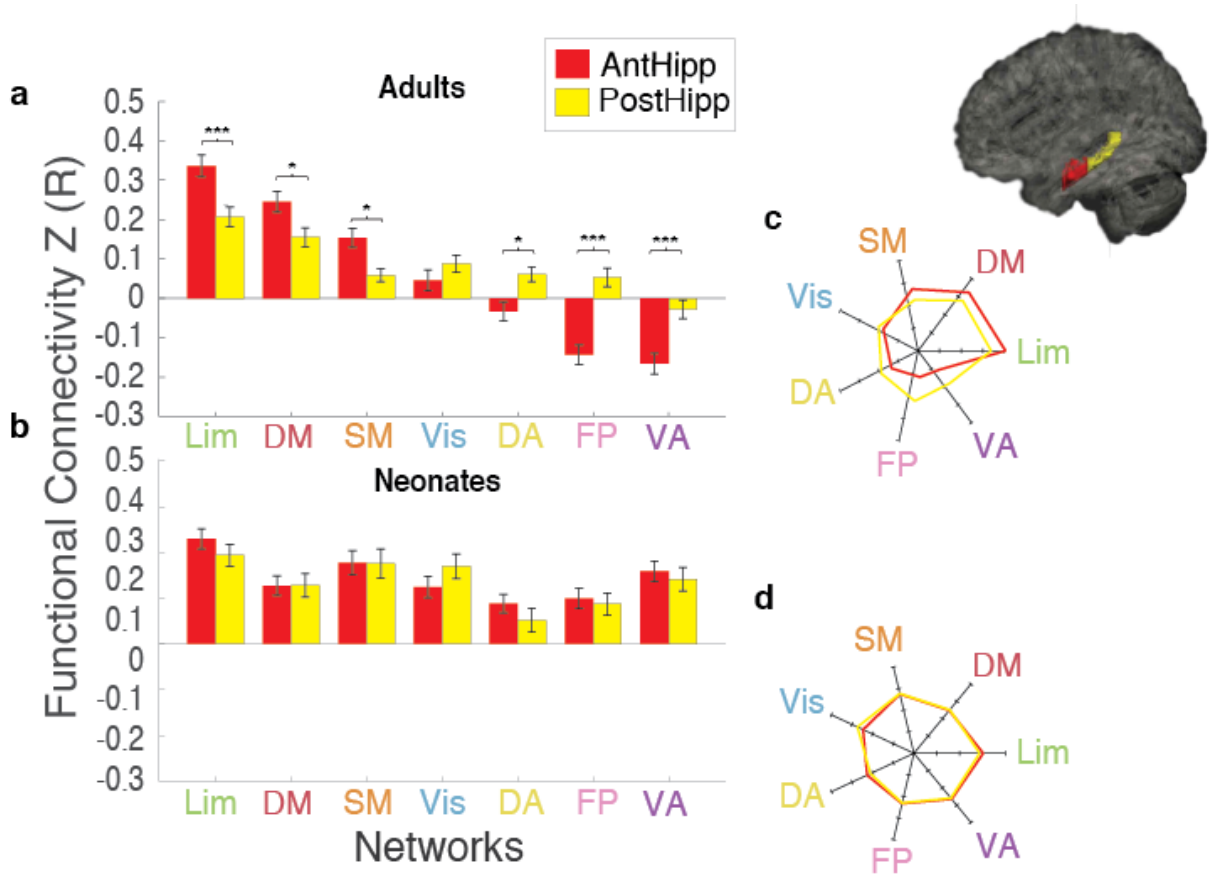
a
Adults
AntHipp
PostHipp
Functional Connectivity Z (R)
0.5
0.4
0.3
0.2
0.1
0
-0.1
-0.2
-0.3
Lim DM SM Vis DA FP VA
b
Neonates
Networks
c
d
SM
DM
Vis
Lim
DA
FP
VA

(Figure 4)

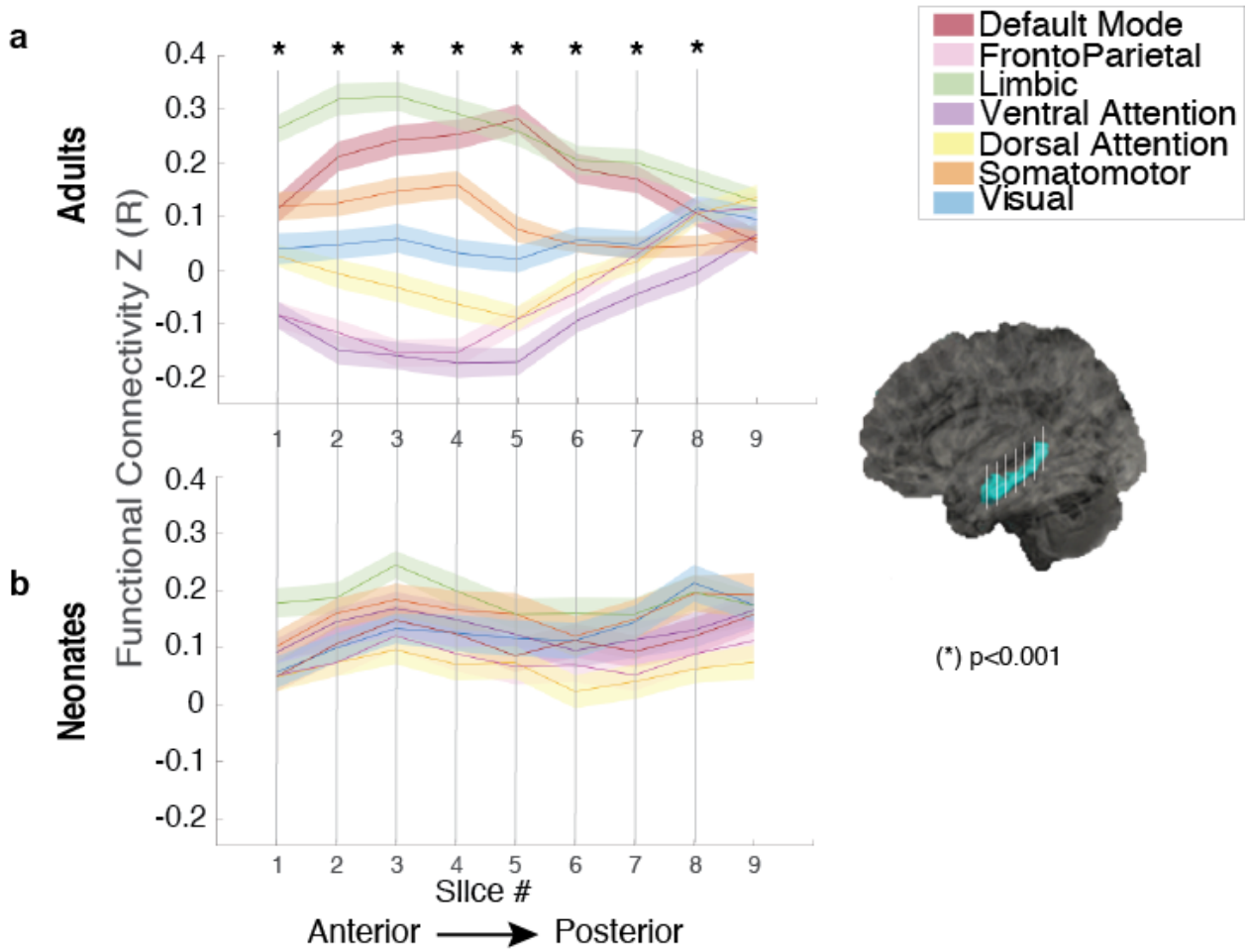
a
b
Adults
Neonates
Functional Connectivity Z (R)
0.4
0.3
0.2
0.1
0
-0.1
-0.2
1 2 3 4 5 6 7 8 9
Slice #
Anterior
Posterior
Default Mode
FrontoParietal
Limbic
Ventral Attention
Dorsal Attention
Somatomotor
Visual
(*) p<0.001

(Figure 5)